



**HAL**  
open science

## An insight into REEs recovery from spent fluorescent lamps: Evaluation of the affinity of an NH<sub>4</sub>-13X zeolite towards Ce, La, Eu and Y

Francesco Colombo, Riccardo Fantini, Francesco Di Renzo, Gianluca Malavasi, Daniele Malferrari, Rossella Arletti

### ► To cite this version:

Francesco Colombo, Riccardo Fantini, Francesco Di Renzo, Gianluca Malavasi, Daniele Malferrari, et al.. An insight into REEs recovery from spent fluorescent lamps: Evaluation of the affinity of an NH<sub>4</sub>-13X zeolite towards Ce, La, Eu and Y. *Waste Management*, 2024, 175, pp.339-347. 10.1016/j.wasman.2024.01.023 . hal-04591515

**HAL Id: hal-04591515**

**<https://hal.science/hal-04591515>**

Submitted on 28 May 2024

**HAL** is a multi-disciplinary open access archive for the deposit and dissemination of scientific research documents, whether they are published or not. The documents may come from teaching and research institutions in France or abroad, or from public or private research centers.

L'archive ouverte pluridisciplinaire **HAL**, est destinée au dépôt et à la diffusion de documents scientifiques de niveau recherche, publiés ou non, émanant des établissements d'enseignement et de recherche français ou étrangers, des laboratoires publics ou privés.

1 **An insight into REEs recovery from spent fluorescent lamps: evaluation of the affinity of an NH<sub>4</sub>-**  
2 **13X zeolite towards Ce, La, Eu and Y**

3

4 Francesco Colombo<sup>a</sup>, Riccardo Fantini<sup>a</sup>, Francesco Di Renzo<sup>b</sup>, Gianluca Malavasi<sup>a</sup>, Daniele  
5 Malferrari<sup>a</sup>, Rossella Arletti<sup>a</sup>

6

7 corresponding author: Rossella Arletti rossella.arletti@unimore.it

8

9 <sup>a</sup>*Dipartimento di Scienze Chimiche e Geologiche, Università degli Studi di Modena e Reggio Emilia,*  
10 *Modena, Italy*

11 <sup>b</sup>*ICGM, University of Montpellier, CNRS, ENSCM, Place Eugène Bataillon, 34095, Montpellier,*  
12 *France*

13 **Abstract:** The constantly increasing demand of Rare Earth Elements (REEs) made them to be part  
14 of the so-called “critical elements” indispensable for the energy transition. The monopoly of only a  
15 few countries, the so-called balance problem between demand and natural abundance, and the  
16 need to limit the environmental costs of their mining, stress the necessity of a recycling policy of  
17 these elements. Different methods have been tested for REEs recovery. Despite the well-known  
18 ion-exchange properties of zeolites, just few preliminary works investigated their application for  
19 REEs separation and recycle. In this work we present a double ion exchange experiment on a NH<sub>4</sub>-  
20 13X zeolite, aimed at the recovery of different REEs from solutions mimicking the composition of  
21 liquors obtained from the leaching of spent fluorescent lamps.

22 The results showed that the zeolite was able to exchange all the REEs tested, but the exchange  
23 capacity was different: despite Y being the more concentrated REE in the solutions, the cation  
24 exchange was lower than less concentrated ones (16 atoms p.u.c. vs 21 atoms for Ce and La

25 solutions), suggesting a possible selectivity. In order to recover REEs from the zeolite, a second  
26 exchange with an ammonium solution was performed. The analyses of the zeolites show that  
27 almost all of Ce and Eu remain in the zeolite, while nearly half of La and Y are released. This, once  
28 again, suggests a possible selective release of REEs and open the possibility for a recovery process  
29 in which Rare Earths can be effectively separated.

30 **Keywords:** Zeolite X, Cation exchange, REE, recovery

31

## 32 **1. Introduction**

33 Rare Earth Elements (REEs) are a group of seventeen elements, fifteen of which are the  
34 Lanthanides with the addition of scandium and yttrium. Their demand is constantly increasing due  
35 to their extensive use in many technological applications such as computer memory, DVDs,  
36 rechargeable batteries, autocatalytic converters, super magnets, mobile phones, LED lighting,  
37 superconductors, glass additives, fluorescent materials, phosphate binding agents, solar panels  
38 and magnetic resonance imaging (MRI) agents (Balaram, 2019).

39 An European foresight study on Critical Raw Materials (Bobba et al., 2020) shows how REEs are  
40 part of a group of raw materials fundamental for the energy transition. The report displays how  
41 the use of some REEs for the mentioned technologies will more than double from 2030 to 2050.  
42 The risk in the supply of these elements is higher than others because they have a very high  
43 demand rate against the number of known ores. Moreover, as reported in the study, the REEs  
44 market is mastered by China which is the world's largest producer, consumer, and exporter of  
45 REEs (e.g., the 98% of the EU's supply of REEs is provided by China). To achieve resource security,  
46 it is crucial to diversify the supply from primary and secondary sources enabling reduced  
47 dependency on a single country and, most importantly, improving resource efficiency and  
48 circularity (European Commission, 2020).

49 A lot of work has been done to find and characterize REEs-rich waste materials from which to  
50 recover these elements; among them, phosphogypsum, red muds (bauxite processing residue),  
51 mine tailings, coal and incinerator ashes, metallurgical slags, wastewater and different electronic  
52 and electrical equipment wastes (WEEE) have been identified as suitable candidates (Binnemans  
53 et al., 2015). Phosphogypsum, the calcium sulfate hydrated waste from the production of  
54 phosphate fertilizers, occurs in large quantities and can contain a lot of different REEs, mainly  
55 depending on the source rock (Cánovas et al., 2019); moreover, it may also contain radionuclides,  
56 making it a material of environmental and health concern. The concentration of REEs in red muds  
57 depend strongly on the lithologies of the bauxite host-rock (Borra et al., 2016) which can be of  
58 three types: Tikhvin-type bauxites (0.5 %) lying on aluminosilicate rocks, the “classical” lateritic  
59 bauxites (88 %) and karst bauxites (11.5 %), deposits lying on carbonates which may contain the  
60 highest amounts of REEs. Waste materials like acid mine drainage (AMD) (Ayora et al., 2016;  
61 González et al., 2020; Hedin et al., 2019; Li and Wu, 2017), mine tailings (Zhang et al., 2014) and  
62 ashes (Blissett et al., 2014; Funari et al., 2016) have a REEs concentration strongly related to the  
63 primary material, thus each case study requires a proper evaluation.

64 WEEEs comprehend, among others, NdFeB magnets, Ni-MH batteries, and phosphors from  
65 fluorescent lamps. NdFeB magnets contain about 31-32 wt% of REEs (Yang et al., 2017). The  
66 content of REEs in spent NiMH batteries is approximately 90 mg/kg for La, 27 mg/kg for Ce and 26  
67 mg/kg for Nd (Lie and Liu, 2021), and they also contain fair amounts of Mn, Co, Zn, Cd and Al.  
68 Fluorescent lamps are based on different phosphor types: white phosphor (HALO), red phosphor  
69 (YOX), green phosphors (LAP, CAT and CBT) and blue phosphor. HALO does not contain REEs, while  
70 in the others Y, Eu, La, Ce, Tb and Gd occur (Gijsemans et al., 2018). A major requirement of  
71 WEEEs recycling is to previously optimize their physical dismantling and concentration in  
72 diversified scraps (Jowitt et al., 2018). As the separation of different phosphor types is rarely

73 achieved in this process, the recovery of REEs requires their selective separation from a common  
74 leaching solution, generally obtained after a series of physicochemical processes aimed at the  
75 beneficiation of REEs (Ambaye et al., 2020; Xie et al., 2023; Yuksekdog et al., 2022). An effective  
76 separation can be achieved through various methods. For example, a selective precipitation can be  
77 done through different reagents favouring the precipitation of double salts, hydroxides, oxalates  
78 and carbonates (Mao et al., 2022; Pavón et al., 2018; Porvali et al., 2018; Silva et al., 2019). Solvent  
79 extraction, or liquid-liquid extraction is highly used and is commercially exploited to produce high  
80 purity single REEs; however, it is an inefficient, labour-intensive and time-consuming method  
81 (Opare et al., 2021). Adsorption of REEs can also be carried out with either organic or inorganic  
82 compounds, depending on the element considered; the effectiveness of this method is strongly  
83 related to contact time, adsorbent dose, initial concentration, solution pH and temperature  
84 (Anastopoulos et al., 2016; Iannicelli-Zubiani et al., 2015; Pinto et al., 2023). Ion exchange is  
85 another widely exploited method that is generally carried out exploiting different resins (Chen et  
86 al., 2017; Hérès et al., 2018) and MOFs.

87 Zeolites are a family of microporous materials, natural and synthetic, which are classified  
88 according to their structure (framework types) and chemism. Zeolites are usually exploited for  
89 their cation exchange property which mainly depend on the  $Al^{3+}$  for  $Si^{4+}$  substitutions in  
90 tetrahedra. The REEs adsorption on zeolite faujasite (framework type FAU) (Baerlocher et al.,  
91 2007) from concentrated solutions has been extensively studied, notably but not exclusively for  
92 the preparation of fluid catalytic cracking (FCC) (Chen et al., 1990; Guzzinati et al., 2018). Despite  
93 this, only few studies evaluated the possible exploitation of zeolites for the recovery of REEs  
94 (Barros et al., 2019; Confalonieri et al., 2022; Eremin et al., 2017; Kocasoy and Şahin, 2007; Mosai  
95 et al., 2019; Mosai and Tutu, 2021; Motsi et al., 2009).

96 The use of zeolites as cation exchangers in the acidic conditions typical of mineral extraction  
97 processes can be limited by the acid hydrolysis of the Si-O-Al bonds, easier for Al-rich zeolites. This  
98 has prompted experimentation on natural (clinoptilolite) or synthetic (zeolite-L (LTL)) zeolites, with  
99 a relatively high Si/Al ratio. The cheapest synthetic zeolites, like zeolite-A (LTA) and faujasite (FAU),  
100 are produced with a low Si/Al ratio, slightly above unity, which gives a very high ion exchange  
101 capacity; nevertheless, these materials are more prone to dealumination and amorphization in  
102 acidic solution than those with higher Si/Al ratios.

103 The aim of this work is to evaluate the extent to which instability in acid solution is limiting for the  
104 use of low Si/Al zeolites in REE recovery. The cation exchange capacity of a synthetic  $\text{NH}_4$   
105 exchanged 13X zeolite (FAU framework type) (Baerlocher et al., 2007) was studied against four  
106 different rare earth elements (Ce, La, Eu and Y) and the recovery of the exchanged REEs was also  
107 evaluated. Solution concentrations were chosen by mimicking those resulting from a two-step  
108 leaching on spent fluorescent lamps with hydrochloric acid (Eduafo et al., 2015).

## 110 **2. Materials and Methods**

### 112 **2.1 $\text{NH}_4$ -13X zeolite**

113 As will be better detailed below, an  $\text{NH}_4$  saturated zeolite was prepared to test the counter-  
114 exchange of  $\text{NH}_4$  for the recovery of the REEs from a solution containing only REEs and readily  
115 removable ammonium.

116 Molecular Sieve 13X is the sodium form of synthetic zeolite X, and it is characterized by a low Si/Al  
117 ratio, high porosity, and high cation exchange capacity of 300 meq/100g (Mondale et al., 1995;  
118 Rees, 1970). One of the main properties of this material is its great ability to exchange cations. This  
119 zeolite is characterized by the primary building block SOD (*i.e.* sodalite cage) (Supplementary

120 Figure 1) and cages are connected by double six-rings to form accessible larger cavities (Baerlocher  
121 et al., 2007; Zhu and Seff, 1999).

122 Starting from the 13X zeolite of BDH Chemicals Ltd Poole England, about 30 grams of  $\text{NH}_4$   
123 exchanged 13X form was prepared by putting 4g of zeolite in contact with 1L of a 0.5M  $\text{NH}_4\text{Cl}$   
124 solution (Carlo Erba analytical grade reagent), under stirring, for 24h at room temperature; zeolite  
125 was then separated from the solution via filtration (Filter: Cat No 1005125, Whatman), washed  
126 three times with MilliQ and dried at 60°C.

127 Major elements composition was determined by WDS-XRF (Wavelength-Dispersive Spectrometer  
128 X-ray Fluorescence) Philips PW1480, while ammonium and water content were measured by TGA  
129 (Thermogravimetric Analyses) with a Seiko SSC/5200 thermal analyser in air flow, with heating  
130 range and gradient 25-1050°C and 10°C/min, respectively. The chemical formula of the obtained  
131 material is  $(\text{NH}_4)_{55.5} \text{Na}_{24.7} \text{Mg}_{0.8} \text{Ca}_{0.06} \text{Ti}_{0.02} \text{Fe}_{0.04} \text{Al}_{90.6} \text{Si}_{103.5} \text{O}_{384} \times 205 \text{H}_2\text{O}$ .

132

## 133 **2.2 13X stability tests**

134 To assess whether the 13X zeolite maintains the crystallinity during the REE-exchange procedure,  
135 preliminary stability tests were performed by interacting the zeolite with HCl solutions at the pH  
136 value of 4.4 for 24h at room temperature. Treated zeolite was separated by centrifugation (8000  
137 rpm, 5 min.), washed three times with MilliQ water and then dried at 60°C. A second stability test  
138 was then performed with the same procedure on the material recovered after the first test at pH  
139 4.4, to evaluate the possibility of zeolite re-use for more exchange cycles. The occurrence of  
140 amorphous material was then evaluated on X-ray powder diffraction (XRPD) patterns collected  
141 with an X'Pert PRO diffractometer and analysed by applying the Rietveld - RIR method using GSAS  
142 software (Larson and Dreele, 2000) and methods described in Gualtieri (2000) and Gualtieri et al.  
143 (2019).

144

### 145 **2.3 REEs exchange tests**

146 Four single-element solutions mimicking the concentrations found in leaching solutions of  
147 fluorescent lamps (Ce 0.03M, La 0.04M, Eu 0.006M and Y 0.17M) (Eduafo et al., 2015) were  
148 prepared. For Ce and La cation exchange tests proper amounts of  $\text{Ce}(\text{NO}_3)_3 \cdot 6\text{H}_2\text{O}$  (99%, Aldrich)  
149 and  $\text{La}(\text{NO}_3)_3 \cdot 6\text{H}_2\text{O}$  (99.9%, Alfa Aesar) were dissolved in MilliQ with a final pH of 4.66 and 4.33,  
150 respectively. For Eu and Y cation exchange tests,  $\text{Eu}_2\text{O}_3$  (99.9%, Aldrich) and  $\text{Y}_2\text{O}_3$  (99.9%, Alfa  
151 Aesar) were dissolved in MilliQ with the addition of  $\text{HNO}_3$  (Carlo Erba, analytical grade reagent),  
152 obtaining a final pH of 2.67 and 1.55, respectively. Since pH values below 4 can induce zeolites  
153 dealumination and/or amorphization, while pH values higher than 5 can lead to REE precipitation  
154 (Han, 2020), TRIS (tris(hydroxymethyl)aminomethane, 99.9%, Aldrich) was used to buffer the pH at  
155 about 4.4 for both the Eu and Y solutions.

156 The REEs exchange tests were performed by putting the  $\text{NH}_4$ -13X zeolite in contact with the single-  
157 element REE solutions under stirring for 24h at room temperature using three different liquid-to-  
158 solid (l/s) ratios: 10/1, 50/1 and 100/1 ml/g. The zeolites were then separated from the solutions  
159 by centrifugation (8000 rpm, 5 min.), washed three times with MilliQ water and dried at 60°C. The  
160 solutions, once separated from the zeolite, were filtered with a 0.45  $\mu\text{m}$  filter. Elemental Analyses  
161 (FLASH 2000 CHNS Analyzer) were performed to evaluate the nitrogen content in zeolite samples  
162 in "FLASH" dynamic combustion (modified Dumas' method), a method that allows to heat sample  
163 at 1800 °C and analyse the released elementary gases, separated through a chromatographic  
164 column, using a highly sensitive thermal conductivity (TCD) detector. SEM-EDS analysis were  
165 performed on REE exchanged zeolites powders compressed into thin discs and coated with  
166 carbon. Thermogravimetric characterization was carried out applying the same experimental  
167 conditions used for  $\text{NH}_4$ -13X zeolite.



168 The final exchange solutions were analysed by inductively coupled plasma optical emission  
169 spectroscopy (ICP-OES) Perkin Elmer Optima 4200 DV to evaluate the content of Ce, La, Eu and Y  
170 (Supplementary Table 2). The pH of the solutions was measured at the beginning of the exchange  
171 test, after 1h, 2h, 20h, 22h and 24h, data are reported in Supplementary Table 3.

172

## 173 **2.4 REEs recovery from zeolite**

174 In order to recover REEs from the exchanged zeolites, REEs were extracted by a further exchange  
175 with a 0.8M NH<sub>4</sub>Cl solution. The REEs enriched zeolites were put in contact with the solution for  
176 24h at room temperature under stirring, using a solid/liquid ratio of 1/125 g/ml. The zeolite  
177 powders were then separated from the solution and characterized as described above.

178

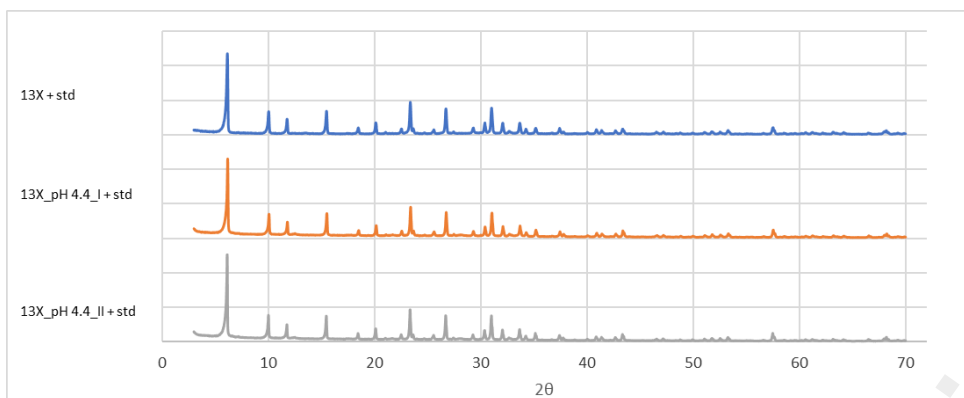
## 179 **3. Results and discussion**

180

### 181 **3.1 pH stability tests**

182 Stability tests at pH 4.4 (Supplementary Table 1) showed a considerable increase in amorphous  
183 content after the first treatment (24h), while no significant changes occurred after the second  
184 treatment. It is therefore possible to assume that the amorphization stabilised at less than 30 wt%.  
185 The amorphization could derive from zeolite dealumination and the consequent precipitation of  
186 EFAL (extra-framework aluminium species) on the surface and inside the porosity of the zeolite  
187 (Janssen et al., 2001). The XRPD patterns of the sample before and after pH tests do not show  
188 other major differences (Figure 1).

189



190

191

192 *Figure 1. XRPD pattern of the samples before and after the pH test. 10 wt% of corundum was*  
 193 *added to the samples as internal standard (std in labels) to calculate the amount of amorphous*  
 194 *material.*

195

### 196 **3.2 REEs exchange of NH<sub>4</sub>-13X**

197 NH<sub>4</sub>-13X samples were put in contact with different volumes of solutions having concentration of  
 198 each REE chosen as typical of the effluent of WEEE waste acid leaching (Eduafo et al., 2015).

199 Liquid-to-solid ratios of 10, 50 and 100 ml/g were used, and the concentrations of the solutions  
 200 were 0.029, 0.037, 0.005 and 0.13 for Ce, La, Eu and Y, respectively (Supplementary Table 2). The  
 201 composition of the initial 13X and of the REE-exchanged zeolites are reported in Supplementary  
 202 Table 4, while the calculated chemical formulas are given in Table 1.

203

Sample	Chemical Formula	C. U. [%]
NH <sub>4</sub> -13X	(NH <sub>4</sub> ) <sub>55.48</sub> Na <sub>24.73</sub> Mg <sub>0.83</sub> Ca <sub>0.06</sub> Ti <sub>0.02</sub> Fe <sub>0.04</sub> Al <sub>90.65</sub> Si <sub>103.47</sub> O <sub>384</sub> × 206 H <sub>2</sub> O	11.53
NH <sub>4</sub> -13X_Ce0.03M_1/10	Ce <sub>5.61</sub> (NH <sub>4</sub> ) <sub>40.98</sub> Na <sub>17.57</sub> Al <sub>85.95</sub> Si <sub>108.69</sub> O <sub>384</sub> × 250.27 H <sub>2</sub> O	12.29
NH <sub>4</sub> -13X_Ce0.03M_1/50	Ce <sub>21.02</sub> (NH <sub>4</sub> ) <sub>12.59</sub> Na <sub>9.6</sub> Al <sub>86.81</sub> Si <sub>105.57</sub> O <sub>384</sub> × 276.87 H <sub>2</sub> O	1.79
NH <sub>4</sub> -13X_Ce0.03M_1/100	Ce <sub>22.88</sub> (NH <sub>4</sub> ) <sub>10.2</sub> Na <sub>9.29</sub> Al <sub>85.08</sub> Si <sub>106.20</sub> O <sub>384</sub> × 280.19 H <sub>2</sub> O	-3.39
NH <sub>4</sub> -13X_La0.04M_1/10	La <sub>6.93</sub> (NH <sub>4</sub> ) <sub>36.51</sub> Na <sub>17.06</sub> Al <sub>85.75</sub> Si <sub>109.10</sub> O <sub>384</sub> × 252.61 H <sub>2</sub> O	13.30

<i>NH<sub>4</sub>-13X_La0.04M_1/50</i>	La <sub>21.93</sub> (NH <sub>4</sub> ) <sub>11.35</sub> Na <sub>8.29</sub> Al <sub>85.65</sub> Si <sub>106.04</sub> O <sub>384</sub> × 277.62 H <sub>2</sub> O	0.26
<i>NH<sub>4</sub>-13X_La0.04M_1/100</i>	La <sub>20.42</sub> (NH <sub>4</sub> ) <sub>9.52</sub> Na <sub>7.87</sub> Al <sub>85.69</sub> Si <sub>108.07</sub> O <sub>384</sub> × 274.16 H <sub>2</sub> O	8.22
<i>NH<sub>4</sub>-13X_Eu0.006M_1/10</i>	Eu <sub>0.78</sub> (NH <sub>4</sub> ) <sub>52.02</sub> Na <sub>19.18</sub> Mg <sub>0.30</sub> P <sub>0.04</sub> Ca <sub>0.12</sub> Al <sub>87.10</sub> Si <sub>107.97</sub> O <sub>384</sub> × 242.49 H <sub>2</sub> O	15.57
<i>NH<sub>4</sub>-13X_Eu0.006M_1/50</i>	Eu <sub>3.82</sub> (NH <sub>4</sub> ) <sub>42.46</sub> Na <sub>17.87</sub> Mg <sub>0.40</sub> P <sub>0.05</sub> Ca <sub>0.08</sub> Al <sub>87.09</sub> Si <sub>108.36</sub> O <sub>384</sub> × 247.56 H <sub>2</sub> O	17.57
<i>NH<sub>4</sub>-13X_Eu0.006M_1/100</i>	Eu <sub>7.64</sub> (NH <sub>4</sub> ) <sub>32.60</sub> Na <sub>17</sub> Mg <sub>0.89</sub> P <sub>0.03</sub> Ca <sub>0.10</sub> Al <sub>87</sub> Si <sub>108.05</sub> O <sub>384</sub> × 254.68 H <sub>2</sub> O	16.64
<i>NH<sub>4</sub>-13X_Y0.17M_1/10</i>	Y <sub>14.11</sub> (NH <sub>4</sub> ) <sub>21.31</sub> Na <sub>17.46</sub> Mg <sub>0.18</sub> P <sub>0.42</sub> Ca <sub>0.11</sub> Al <sub>86.95</sub> Si <sub>105.32</sub> O <sub>384</sub> × 266.51 H <sub>2</sub> O	6.74
<i>NH<sub>4</sub>-13X_Y0.17M_1/50</i>	Y <sub>15.97</sub> (NH <sub>4</sub> ) <sub>16.45</sub> Na <sub>17.51</sub> Mg <sub>0.17</sub> P <sub>0.45</sub> Ca <sub>0.15</sub> Al <sub>87.03</sub> Si <sub>104.98</sub> O <sub>384</sub> × 269.07 H <sub>2</sub> O	5.94
<i>NH<sub>4</sub>-13X_Y0.17M_1/100</i>	Y <sub>16.40</sub> (NH <sub>4</sub> ) <sub>14.25</sub> Na <sub>17.01</sub> Mg <sub>0.47</sub> P <sub>0.61</sub> Ca <sub>0.17</sub> Al <sub>87.17</sub> Si <sub>104.66</sub> O <sub>384</sub> × 271.59 H <sub>2</sub> O	7.70

204

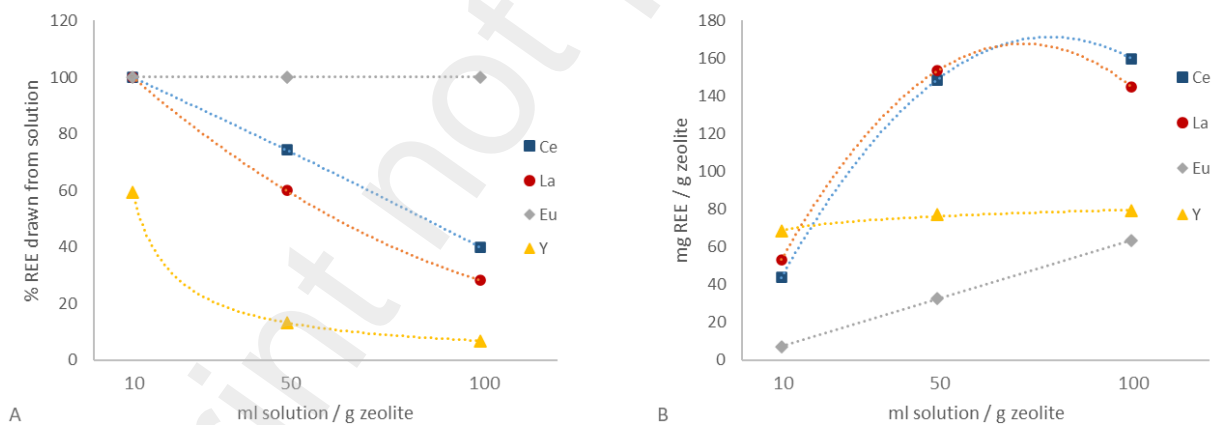
205 *Table 1. Atomic composition of the REE-exchanged zeolites. The charge unbalance (C.U. %) was*  
 206 *calculated with the formula below.*

207 
$$C. U. \% = \frac{Al\ cations - (\Sigma\ monovalent\ cations) - 2 * (\Sigma\ bivalent\ cations) \dots - n * (\Sigma\ n\ valent\ cations)}{Al\ cations} * 100$$

208

209 The fraction of REE extracted from solution is reported in Figure 2A as a function of the liquid-to-  
 210 solid ratio. At a liquid-to-solid ratio of 10 ml/g, virtually all Ce, La, and Eu passes from the solutions  
 211 to the zeolite, while, in the same conditions, only nearly half of Y is extracted from the solution. At  
 212 increasing liquid-to-solid ratio (up to 100 ml/g), Eu is still completely extracted while the fractions  
 213 extracted from Ce, La and Y solutions decreases with the increasing of the solution volume,  
 214 reaching extraction levels of 40, 29 and 7%, respectively for Ce, La and Y, at liquid-to-solid ratio of  
 215 100 mL/g. The REE adsorbed by zeolite increases with the volume of contacting solution (Figure  
 216 2B) with a trend strongly dependent on the initial concentration of the REE solution. The amounts  
 217 of REEs exchanged are reported in mg REE/g zeolite, instead of meq, to give a clearer vision of the  
 218 applicative potential of this recovery process. In the case of the very diluted Eu solution, the  
 219 amount adsorbed is linearly dependent on the volume of solution, reaching a value of 69 mg  
 220 REE/g zeolite at a liquid-to-solid ratio 100 mL/g. The observed linearity suggests that, in these

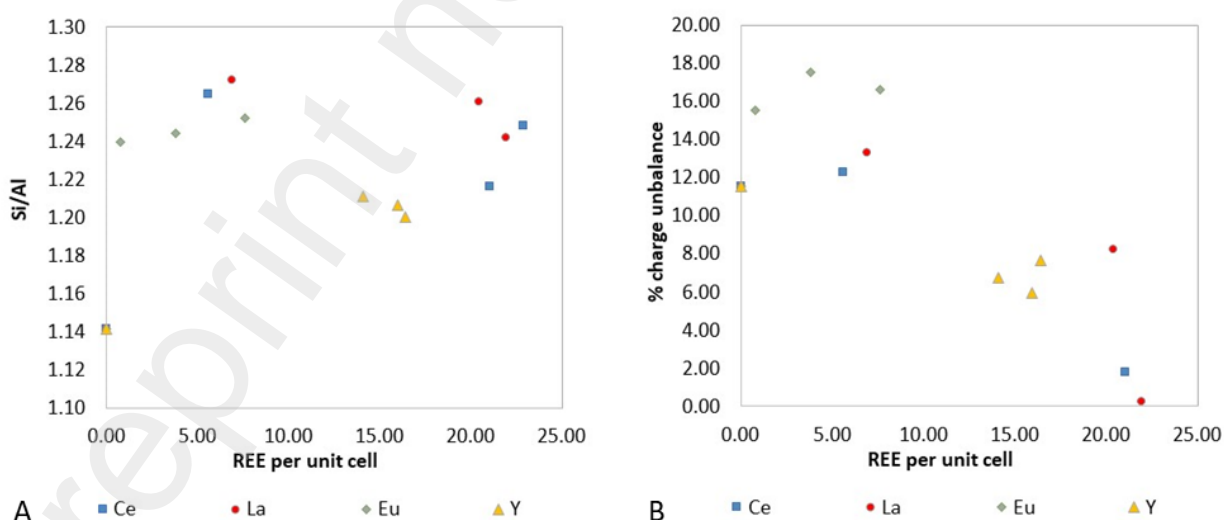
221 experimental conditions, the affinity of Eu for the solution does not depend on the adsorbed  
 222 amount; this trend usually indicates that the adsorbent capacity is far from being saturated. For  
 223 the more concentrated solutions of Ce, La and Y, the adsorbed amount is in the 40-60 mg/g range  
 224 already for 10 ml solution per g of zeolite. At higher liquid-to-solid ratios, the adsorbed amount of  
 225 Ce and La increases nonlinearly with solution volume, reaching values of 135-160 mg/g at liquid-  
 226 to-solid ratio of 50 ml/g. At a liquid-to-solid ratio 100 ml/g the amount of REE incorporated remain  
 227 almost in the same range (150-160 mg/g), indicating the saturation of the zeolite is approaching.  
 228 This behaviour suggests that the affinity of the zeolites for REE cations is decreasing when the  
 229 amount of adsorbed REE is near the saturation capacity of the exchanger. A different response can  
 230 be identified for Y. At higher liquid-to-solid ratios, the amount of Y incorporated in the zeolite  
 231 remains almost the same, indicating that the saturation conditions for Y are reached at the liquid-  
 232 to-solid ratio of 10 ml/g.



234  
 235  
 236 *Figure 2. REE fraction drawn from solution (A) and amount of REE incorporated in the zeolite (B) as*  
 237 *a function of the solid/liquid ratio. Initial concentrations (mg/L): Ce 0.029, La 0.037, Eu 0.005 and Y*  
 238 *0.13. The lines are guides for the eye.*

239

240 The composition of the exchanged zeolites provides some information about their stability; in fact,  
 241 the Si/Al ratio of  $1.23 \pm 0.03$  (Figure 3A) is almost unaffected by the amount of REE in the solid and  
 242 the volume of solution with which the sample interacted. These Si/Al ratios, significantly higher  
 243 than the 1.14 value of the parent 13X, derive from the partial dissolution of Al, as would be  
 244 expected by treating an Al-rich zeolite with an acid solution. The virtual constancy of the Si/Al  
 245 when the solid is treated with larger volumes of acid solution suggests that the extraction of  
 246 aluminium by acid hydrolysis has reached a stable state related to the pH of the solution. The pH  
 247 behaviour of the solution depends on the exchanged REE, initial pH and liquid-to-solid ratio  
 248 (Supplementary Table 3). In general, when the experimental conditions limit  $\text{NH}_4$  exchange, pH  
 249 tend to increase while, high  $\text{NH}_4$  exchange results in a slight decrease in pH. The decrease of pH  
 250 may be due to an increment of  $\text{NH}_4^+$  concentration in the solution that promote acid hydrolysis.  
 251 On the other hand, the increase in pH may be related to a smaller increase of  $\text{NH}_4^+$  concentration  
 252 and to the possible competition between  $\text{H}^+$  protons and REE cations adsorbed in the  $\text{NH}_4$ -13X  
 253 (Sánchez-Hernández et al., 2018), reasonable stabilizing over time at values close to neutrality.  
 254



255  
 256

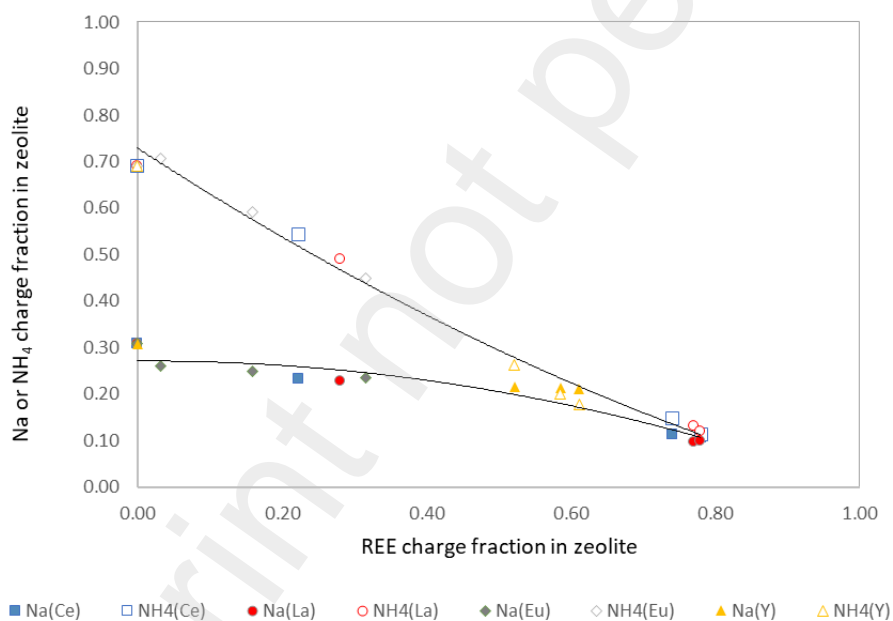
257 *Figure 3. Modification of the zeolite with REE exchange: (A) Si/Al ratio and (B) fraction of Al not*  
258 *contributing to the compensation of the cation charge ((Al-cation charge)/Al) vs. REE cations per*  
259 *unit cell.*

260

261 Hydrolysis of the Al-O-Si bonds passes through the formation of extra-framework aluminium  
262 species (EFAL) which no more form lattice anions whose charge has to be compensated by  
263 exchanged cations. The unbalance between cation charge and aluminium content in the sample,  
264 reported in Figure 3B, provides a first indication on the fraction of aluminium not forming lattice  
265 anions. The pristine 13X already has a significant charge unbalance (about 11 % of Al not requiring  
266 charge compensation), probably due to the presence of amorphous aluminium oxyhydroxides left  
267 over from zeolite synthesis. The charge unbalance of the exchanged samples is strictly related to  
268 their REE content. Samples with low REE content present a larger charge unbalance, suggesting  
269 that the dealumination of the samples has formed EFAL species not dissolved by the acid  
270 treatment. In samples characterized by the highest REE exchange, the charge unbalance  
271 systematically decreases with the REE content. Samples with 20 REE p.u.c. exhibit nearly perfect  
272 charge compensation, suggesting that virtually all aluminium is part of the framework.

273 This effect is probably related to the well-known stabilisation of the faujasite framework by REEs,  
274 which is the basis of the use of REE-Y catalysts in FCC (fluid catalytic cracking) (C. Vogt and  
275 M. Weckhuysen, 2015). Indeed, the highest thermal and hydrothermal stability of REE-exchanged  
276 zeolite Y allowed its use in the high-temperature steam-ridden conditions of the FCC plan  
277 regenerator (Li and Rees, 1986). This lattice stabilisation has been variously attributed to the  
278 polarization effect of REE clusters or REE cations in specific positions in the zeolite cages (Guzman  
279 et al., 2005; Scherzer et al., 1975; Schüßler et al., 2011). This effect was mainly observed for Al-  
280 poor zeolite Y under high-temperature steaming conditions; it is now relevant to observe a similar

281 stabilization also in the REE exchange Al-rich zeolite X in acidic environments. It can also be  
 282 observed that the initial 13X zeolite was not completely in  $\text{NH}_4$  form and a significant amount of  
 283 Na cations were still present. This means that both  $\text{NH}_4^+$  and  $\text{Na}^+$  can be exchanged by REE cations,  
 284 as showed by the results reported in Table 1. The fraction of Na and  $\text{NH}_4$  cations in the exchanged  
 285 zeolites are reported in Figure 4 as a function of the REE charge fraction. It may be noted that the  
 286  $\text{NH}_4$  content decreases nearly linearly with the amount of REE exchanged. The Na fraction takes a  
 287 different trend, remaining almost constant until at least half zeolite anions are compensated by  
 288 REE cations and decreasing only for further REE exchange. This indicates a preferential exchange  
 289 of  $\text{NH}_4$  by REE and, significantly, this trend is common to all REE. Clearly, the affinity of the zeolite  
 290 for REE is much higher than for ammonium, while residual sodium is much less easily exchanged.  
 291



292  
 293 *Figure 4. Na (filled symbols) and  $\text{NH}_4$  (void symbols) content of the exchanged zeolites as a function*  
 294 *of the REE content. Zeolites exchanged with Ce (squares), La (circles), Eu (diamond), Y (triangles).*  
 295 *The lines are polynomial fittings for Na and  $\text{NH}_4$  content.*

296

### 297 3.3 REEs recovery from zeolite

298 The chemical formula and composition of the zeolites after the counter-exchange test in  
 299 ammonium solution are reported in Table 2 and Supplementary Table 4, respectively. The fraction  
 300 of REE extracted from the zeolites by the NH<sub>4</sub> solution vs. the initial amount of REE in the zeolite  
 301 are reported in Figure 5. Two well-defined patterns appear. La and Y can be recovered by cation  
 302 exchange with NH<sub>4</sub><sup>+</sup> at 30-45% while, under the same conditions, Ce and Eu are only recovered at  
 303 10-18% suggesting a higher affinity of the zeolitic framework for the latter two elements. This  
 304 behaviour could be related to the variation of charge unbalance before and after the recovery  
 305 process; in fact, in the case of La and Y the charge unbalance increases after the recovery with a  
 306 consequent release of great amount of charge compensating ions while, in the case of Ce and Eu,  
 307 the variation of charge unbalance before and after the recovery is low, suggesting a major  
 308 stabilization of 13X zeolite after the ionic exchange.

309

<b>Sample</b>	<b>Chemical Formula</b>	<b>C. U. (%)</b>
<i>Ce recovery_1/10</i>	Ce <sub>6.22</sub> (NH <sub>4</sub> ) <sub>55.35</sub> Na <sub>5.94</sub> Mg <sub>0.60</sub> P <sub>0.03</sub> Ca <sub>0.21</sub> Al <sub>86.94</sub> Si <sub>106.33</sub> O <sub>384</sub> x 256.61 H <sub>2</sub> O	8.06
<i>Ce recovery_1/50</i>	Ce <sub>18.23</sub> (NH <sub>4</sub> ) <sub>32.64</sub> Na <sub>2.53</sub> Mg <sub>0.79</sub> P <sub>0.03</sub> Ca <sub>0.11</sub> Al <sub>86.67</sub> Si <sub>104</sub> O <sub>384</sub> x 277.94 H <sub>2</sub> O	-3.69
<i>Ce recovery_1/100</i>	Ce <sub>18.16</sub> (NH <sub>4</sub> ) <sub>31.06</sub> Na <sub>2.59</sub> Mg <sub>1.08</sub> P <sub>0.02</sub> Ca <sub>0.07</sub> Al <sub>87.21</sub> Si <sub>103.93</sub> O <sub>384</sub> x 277.64 H <sub>2</sub> O	-1.07
<i>La recovery_1/10</i>	La <sub>4.93</sub> (NH <sub>4</sub> ) <sub>48.37</sub> Na <sub>5.08</sub> P <sub>0.04</sub> Al <sub>86.24</sub> Si <sub>110.16</sub> O <sub>384</sub> x 258.17 H <sub>2</sub> O	20.86
<i>La recovery_1/50</i>	La <sub>11.03</sub> (NH <sub>4</sub> ) <sub>29.98</sub> Na <sub>2.28</sub> Mg <sub>0.45</sub> P <sub>0.08</sub> Ca <sub>0.08</sub> Al <sub>88.53</sub> Si <sub>108.79</sub> O <sub>384</sub> x 260.86 H <sub>2</sub> O	26.18
<i>La recovery_1/100</i>	La <sub>11.38</sub> (NH <sub>4</sub> ) <sub>29.77</sub> Na <sub>2.41</sub> Mg <sub>0.33</sub> P <sub>0.02</sub> Al <sub>88.21</sub> Si <sub>109.05</sub> O <sub>384</sub> x 260.98 H <sub>2</sub> O	24.79
<i>Eu recovery_1/10</i>	Eu <sub>0.68</sub> (NH <sub>4</sub> ) <sub>61.27</sub> Na <sub>8.5</sub> Mg <sub>0.41</sub> P <sub>0.01</sub> Ca <sub>0.10</sub> Al <sub>86.25</sub> Si <sub>109.09</sub> O <sub>384</sub> x 254.16 H <sub>2</sub> O	16.75
<i>Eu recovery_1/50</i>	Eu <sub>3.84</sub> (NH <sub>4</sub> ) <sub>54.83</sub> Na <sub>6.51</sub> Mg <sub>0.43</sub> Ca <sub>0.17</sub> Al <sub>84.60</sub> Si <sub>110.29</sub> O <sub>384</sub> x 266.02 H <sub>2</sub> O	15.14
<i>Eu recovery_1/100</i>	Eu <sub>6.74</sub> (NH <sub>4</sub> ) <sub>47.81</sub> Na <sub>3.93</sub> Mg <sub>0.21</sub> Ca <sub>0.19</sub> Al <sub>88.01</sub> Si <sub>107.80</sub> O <sub>384</sub> x 262.49 H <sub>2</sub> O	18.24
<i>Y recovery_1/10</i>	Y <sub>8.62</sub> (NH <sub>4</sub> ) <sub>43.90</sub> Na <sub>5.96</sub> Mg <sub>0.28</sub> P <sub>0.13</sub> Ca <sub>0.16</sub> Al <sub>86.99</sub> Si <sub>107.29</sub> O <sub>384</sub> x 262.07 H <sub>2</sub> O	12.98
<i>Y recovery_1/50</i>	Y <sub>9.38</sub> (NH <sub>4</sub> ) <sub>42.62</sub> Na <sub>5.13</sub> Mg <sub>0.29</sub> P <sub>0.10</sub> Ca <sub>0.15</sub> Al <sub>86.31</sub> Si <sub>107.83</sub> O <sub>384</sub> x 263.97 H <sub>2</sub> O	12.09



Y recovery\_1/100

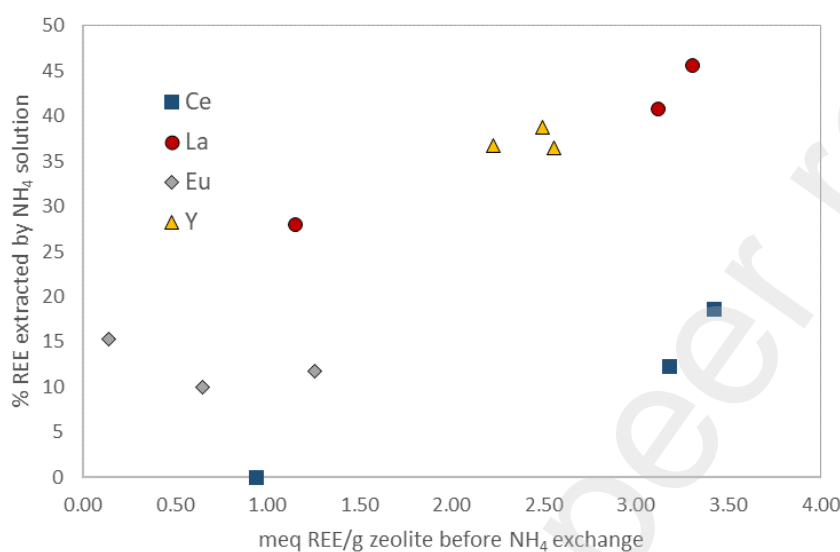
$Y_{10.01} (NH_4)_{41.29} Na_{5.29} Mg_{0.45} P_{0.05} Ca_{0.13} Al_{87.90} Si_{106.51} O_{384} \times 263.77 H_2O$	12.82
---	-------

310

311 *Table 2. Chemical formulas of the REE-exchanged zeolites after ammonium counter exchange. The*

312 *charge unbalance was calculated as described in Table 1.*

313



314

315 *Figure 5. Fraction of REE extracted by ammonium solution as a function of the initial REE content in*

316 *the zeolite.*

317

### 318 **3.4 Exchange isotherms**

319 The affinity of the zeolite for trivalent REE cations is much higher than the affinity for monovalent

320 Na and NH<sub>4</sub>. Therefore, both REE exchange and NH<sub>4</sub> counter-exchange can be used to plot

321 exchange isotherms of REE in 13X. The charge fraction of REE - defined as the ratio charge of REE /

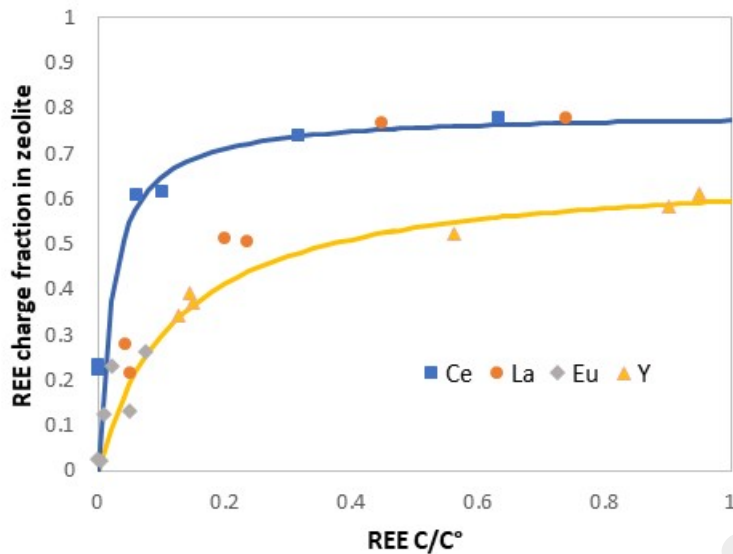
322 the total positive charges - in the zeolite is reported for all samples vs. the relative normality in

323 solution (Figure 6). All exchange isotherms present a sharp rise of exchanged REE at the lowest

324 concentration in solution, confirming the high affinity of REE for the 13X sites. The isotherms show

325 that Ce and La present a saturation plateau at about 0.78 charge fraction, which corresponds to a  
326 capacity of about 66 charges p.u.c. In contrast, yttrium presents a less well-defined plateau at  
327 lower REE content. A lower exchange capacity of 13X for Y than for heavier REE has been already  
328 observed (Guzzinati et al., 2018). The Langmuir isotherm  $q = K * q_{max} * c / (1 + K * c)$ , where  $q$  is the  
329 fraction of exchange sites in the zeolite occupied by REE cations,  $q_{max}$  is the fraction of sites  
330 occupied by REE cations at the saturation of the exchanger,  $K$  is the affinity constant and  $c$  is the  
331  $C/C^\circ$  fraction between REE normality and total cation normality in solution, can be used to verify if  
332 the exchange occurs with the same chemical potential throughout the concentration field. The  
333 isotherms of Ce and Y can be satisfactorily fit by a Langmuir isotherm, suggesting a good  
334 homogeneity of their exchange sites. The  $q_{max}$  values for Ce and Y are very close (0.79 and 0.60 for  
335 Ce and Y, respectively), while the affinity constants significantly differ being 45 and 8, respectively.  
336 In the case of La, the isotherm cannot be fitted by a Langmuir isotherm, suggesting a  
337 heterogeneity of exchange site affinity for REE. However, the trend of the isotherm suggests an  
338 average affinity between those of Ce and Y. In the case of Eu all the experimental points are at  
339 very low  $C/C^\circ$  values and the fitting with an isotherm model cannot be considered reliable.

340



341

342 *Figure 6. Charge fraction of REE in the zeolite vs. REE concentration fraction in equilibrium solution.*

343 *The lines are Langmuir fit of the Ce and Y data.*

344

#### 345 4. Conclusions

346 This research has provided indications on the possible use of zeolites for the recovery of Ce, La and  
347 Y from simulated waste solutions highlighting the strengths and weaknesses of these materials.

348 NH<sub>4</sub>-13X zeolite revealed a good affinity towards REEs. For Ce, La and Y a maximum value of  
349 respectively 23, 22 and 16 atoms p.u.c. exchanged was found, while the starting concentration of  
350 Eu was too low to saturate the zeolite for every liquid-to-solid ratio, and the data obtained are not  
351 sufficient to evaluate the Eu affinity. The best exchange condition in terms of liquid-to-solid ratio  
352 for Ce and La is 50/1: the zeolite reaches amounts of REE p.u.c. near the saturation values, and a  
353 little REE remains in the solution. Y is concentrated enough to already saturate the zeolite also at a  
354 liquid-to-solid ratio of 10/1, yet leaving a lot of REE in the solution. With higher liquid to solid  
355 ratios, either for Ce, La and Y the amount of REE p.u.c. exchanged slightly increase, but not enough

356 to account for the consequent increase of REEs remaining in the solutions. Although Y is the most  
357 concentrated REE in the starting solution (0.13M), it is less exchanged than Ce and La, which were  
358 significantly less concentrated (respectively 0.03M and 0.04M). While Ce and La have a similar  
359 behaviour in exchanging with  $\text{NH}_4$  and the residual Na, Y exchanges  $\text{NH}_4$  in the same way, but is  
360 unable to exchange Na like Ce and La. Ce and La have therefore a higher affinity for the zeolite  
361 than both  $\text{NH}_4$  and Na, while Y is more affine than  $\text{NH}_4$  but less than Na. This could be due to the  
362 significantly smaller ionic radius of Y with respect to that of Ce, La and Na, suggesting that zeolite  
363  $\text{NH}_4$ -13X is selective toward REEs with larger ionic radii. For applicative purposes, the Na remaining  
364 in the zeolite can thus play a relevant role; therefore, further experiments should be aimed at the  
365 total removal of Na from the zeolite before the REE-exchange tests, in order to evaluate the  
366 variations of the affinities in a fully  $\text{NH}_4$ -exchanged 13X.

367 The recovery of REEs from the exchanged zeolites is another aspect to work on. Ce and Eu  
368 recoveries were almost nil, while almost half of La and Y were recovered. With a view to the work  
369 of Eduafo et al. (2015), from which the concentrations of the starting solutions were taken, these  
370 findings are crucial. In fact, considering that this behaviour was observed by the interaction with  
371 two different solutions, one enriched in Ce and La and the other one in Eu and Y,  $\text{NH}_4$ -13X zeolite  
372 can potentially selectively release La over Ce and Y over Eu.

373

## 374 5. References

375

376 Ambaye, T.G., Vaccari, M., Castro, F.D., Prasad, S., Rtimi, S., 2020. Emerging technologies for the  
377 recovery of rare earth elements (REEs) from the end-of-life electronic wastes: a review on  
378 progress, challenges, and perspectives. *Environ. Sci. Pollut. Res.* 27, 36052–36074.

379 <https://doi.org/10.1007/s11356-020-09630-2>

380 Anastopoulos, I., Bhatnagar, A., Lima, E.C., 2016. Adsorption of rare earth metals: A review of  
381 recent literature. *J. Mol. Liq.* 221, 954–962. <https://doi.org/10.1016/j.molliq.2016.06.076>

382 Ayora, C., Macías, F., Torres, E., Lozano, A., Carrero, S., Nieto, J.-M., Pérez-López, R., Fernández-  
383 Martínez, A., Castillo-Michel, H., 2016. Recovery of Rare Earth Elements and Yttrium from  
384 Passive-Remediation Systems of Acid Mine Drainage. *Environ. Sci. Technol.* 50, 8255–8262.  
385 <https://doi.org/10.1021/acs.est.6b02084>

386 Baerlocher, C., McCusker, L.B., Olson, D., Meier, W.M., 2007. Atlas of zeolite framework types, 6th  
387 rev. ed. ed. Published on behalf of the Structure Commission of the International Zeolite  
388 Association by Elsevier, Amsterdam Boston.

389 Balaram, V., 2019. Rare earth elements: A review of applications, occurrence, exploration,  
390 analysis, recycling, and environmental impact. *Geosci. Front.* 10, 1285–1303.  
391 <https://doi.org/10.1016/j.gsf.2018.12.005>

392 Barros, Ó., Costa, L., Costa, F., Lago, A., Rocha, V., Vipotnik, Z., Silva, B., Tavares, T., 2019. Recovery  
393 of rare earth elements from wastewater towards a circular economy. *Molecules* 24.  
394 <https://doi.org/10.3390/molecules24061005>

395 Binnemans, K., Jones, P.T., Blanpain, B., Van Gerven, T., Pontikes, Y., 2015. Towards zero-waste  
396 valorisation of rare-earth-containing industrial process residues: A critical review. *J. Clean.  
397 Prod.* 99, 17–38. <https://doi.org/10.1016/j.jclepro.2015.02.089>

398 Blissett, R.S., Smalley, N., Rowson, N.A., 2014. An investigation into six coal fly ashes from the  
399 United Kingdom and Poland to evaluate rare earth element content. *Fuel* 119, 236–239.  
400 <https://doi.org/10.1016/j.fuel.2013.11.053>

401 Bobba, S., Carrara, S., Huisman, J., Mathieux, F., Pavel, C., 2020. Critical raw materials for strategic  
402 technologies and sectors in the EU. A Foresight Study.

- 403 Borra, C.R., Blanpain, B., Pontikes, Y., Binnemans, K., Van Gerven, T., 2016. Recovery of Rare Earths  
404 and Other Valuable Metals From Bauxite Residue (Red Mud): A Review. *J. Sustain. Metall.*  
405 2, 365–386. <https://doi.org/10.1007/s40831-016-0068-2>
- 406 Cánovas, C.R., Chapron, S., Arrachart, G., Pellet-Rostaing, S., 2019. Leaching of rare earth elements  
407 (REEs) and impurities from phosphogypsum: A preliminary insight for further recovery of  
408 critical raw materials. *J. Clean. Prod.* 219, 225–235.  
409 <https://doi.org/10.1016/j.jclepro.2019.02.104>
- 410 Chen, P., Yang, F., Liao, Q., Zhao, Z., Zhang, Y., Zhao, P., Guo, W., Bai, R., 2017. Recycling and  
411 separation of rare earth resources lutetium from LYSO scraps using the diglycol amic acid  
412 functional XAD-type resin. *Waste Manag.* 62, 222–228.  
413 <https://doi.org/10.1016/j.wasman.2017.02.020>
- 414 Chen, S.H., Chao, K.J., Lee, T.Y., 1990. Lanthanum-NaY zeolite ion exchange. 1. Thermodynamics  
415 and thermochemistry. *Ind. Eng. Chem. Res.* 29, 2020–2023.  
416 <https://doi.org/10.1021/ie00106a007>
- 417 Confalonieri, G., Vezzalini, G., Maletti, L., Di Renzo, F., Gozzoli, V., Arletti, R., 2022. Ion exchange  
418 capacity of synthetic zeolite L: a promising way for cerium recovery. *Environ. Sci. Pollut.*  
419 *Res.* 29, 65176–65184. <https://doi.org/10.1007/s11356-022-20429-1>
- 420 C. Vogt, E.T., M. Weckhuysen, B., 2015. Fluid catalytic cracking: recent developments on the grand  
421 old lady of zeolite catalysis. *Chem. Soc. Rev.* 44, 7342–7370.  
422 <https://doi.org/10.1039/C5CS00376H>
- 423 Eduafo, P.M., Strauss, M.L., Mishra, B., 2015. Experimental investigation of recycling rare earth  
424 metals from waste fluorescent lamp phosphors. Presented at the TMS Annual Meeting, pp.  
425 253–259. <https://doi.org/10.1002/9781119093244.ch29>

426 Eremin, O.V., Epova, E.S., Filenko, R.A., Rusal', O.S., Bychinsky, V.A., 2017. Use of Zeolite Rocks in  
427 Metal Recovery from Mine Water. *J. Min. Sci.* 53, 915–924.  
428 <https://doi.org/10.1134/S1062739117052957>

429 European Commission, 2020. Critical raw materials resilience: Charting a path towards greater  
430 security and sustainability. [https://eur-lex.europa.eu/legal-](https://eur-lex.europa.eu/legal-content/EN/TXT/?uri=CELEX:52020DC0474)  
431 [content/EN/TXT/?uri=CELEX:52020DC0474](https://eur-lex.europa.eu/legal-content/EN/TXT/?uri=CELEX:52020DC0474)

432 Funari, V., Bokhari, S.N.H., Vigliotti, L., Meisel, T., Braga, R., 2016. The rare earth elements in  
433 municipal solid waste incinerators ash and promising tools for their prospecting. *J. Hazard.*  
434 *Mater.* 301, 471–479. <https://doi.org/10.1016/j.jhazmat.2015.09.015>

435 Gijsemans, L., Forte, F., Onghena, B., Binnemans, K., 2018. Recovery of rare earths from the green  
436 lamp phosphor LaPO<sub>4</sub>:Ce<sup>3+</sup>,Tb<sup>3+</sup> (LAP) by dissolution in concentrated methanesulphonic  
437 acid. *RSC Adv.* 8, 26349–26355. <https://doi.org/10.1039/c8ra04532a>

438 González, R.M., Cánovas, C.R., Olías, M., Macías, F., 2020. Rare earth elements in a historical  
439 mining district (south-west Spain): Hydrogeochemical behaviour and seasonal variability.  
440 *Chemosphere* 253. <https://doi.org/10.1016/j.chemosphere.2020.126742>

441 Gualtieri, A.F., 2000. Accuracy of XRPD QPA using the combined Rietveld-RIR method. *J. Appl.*  
442 *Crystallogr.* 33, 267–278. <https://doi.org/10.1107/S002188989901643X>

443 Gualtieri, A.F., Gatta, G.D., Arletti, R., Artioli, G., Ballirano, P., Cruciani, G., Guagliardi, A.,  
444 Malferrari, D., Masciocchi, N., Scardi, P., 2019. Quantitative phase analysis using the  
445 Rietveld method: towards a procedure for checking the reliability and quality of the results.  
446 *Period. Mineral.* 88. <https://doi.org/10.2451/2019PM870>

447 Guzman, A., Zuazo, I., Feller, A., Olindo, R., Sievers, C., Lercher, J.A., 2005. On the formation of the  
448 acid sites in lanthanum exchanged X zeolites used for isobutane/cis-2-butene alkylation.

449 Microporous Mesoporous Mater. 83, 309–318.  
450 <https://doi.org/10.1016/j.micromeso.2005.04.024>

451 Guzzinati, R., Sarti, E., Catani, M., Costa, V., Pagnoni, A., Martucci, A., Rodeghero, E., Capitani, D.,  
452 Pietrantonio, M., Cavazzini, A., Pasti, L., 2018. Formation of Supramolecular Clusters at the  
453 Interface of Zeolite X Following the Adsorption of Rare-Earth Cations and Their Impact on  
454 the Macroscopic Properties of the Zeolite. *ChemPhysChem* 19, 2208–2217.  
455 <https://doi.org/10.1002/cphc.201800333>

456 Han, K.N., 2020. Characteristics of Precipitation of Rare Earth Elements with Various Precipitants.  
457 *Minerals* 10, 178. <https://doi.org/10.3390/min10020178>

458 Hedin, B.C., Capo, R.C., Stewart, B.W., Hedin, R.S., Lopano, C.L., Stuckman, M.Y., 2019. The  
459 evaluation of critical rare earth element (REE) enriched treatment solids from coal mine  
460 drainage passive treatment systems. *Int. J. Coal Geol.* 208, 54–64.  
461 <https://doi.org/10.1016/j.coal.2019.04.007>

462 Hérès, X., Blet, V., Di Natale, P., Ouattou, A., Mazouz, H., Dhiba, D., Cuer, F., 2018. Selective  
463 extraction of rare earth elements from phosphoric acid by ion exchange resins. *Metals* 8.  
464 <https://doi.org/10.3390/met8090682>

465 Iannicelli-Zubiani, E.M., Cristiani, C., Dotelli, G., Gallo Stampino, P., Pelosato, R., Mesto, E.,  
466 Schingaro, E., Lacalamita, M., 2015. Use of natural clays as sorbent materials for rare earth  
467 ions: Materials characterization and set up of the operative parameters. *Waste Manag.* 46,  
468 546–556. <https://doi.org/10.1016/j.wasman.2015.09.017>

469 Janssen, A.H., Koster, A.J., de Jong, K.P., 2001. Three-Dimensional Transmission Electron  
470 Microscopic Observations of Mesopores in Dealuminated Zeolite Y. *Angew. Chem. Int. Ed.*  
471 40, 1102–1104. [https://doi.org/10.1002/1521-3773\(20010316\)40:6<1102::AID-  
472 ANIE11020>3.0.CO;2-6](https://doi.org/10.1002/1521-3773(20010316)40:6<1102::AID-ANIE11020>3.0.CO;2-6)



473 Jowitt, S.M., Werner, T.T., Weng, Z., Mudd, G.M., 2018. Recycling of the rare earth elements. *Curr.*  
474 *Opin. Green Sustain. Chem., Reuse and Recycling / UN SGDs: How can Sustainable*  
475 *Chemistry Contribute? / Green Chemistry in Education* 13, 1–7.  
476 <https://doi.org/10.1016/j.cogsc.2018.02.008>

477 Kocasoy, G., Şahin, V., 2007. Heavy metal removal from industrial wastewater by clinoptilolite. *J.*  
478 *Environ. Sci. Health - Part ToxicHazardous Subst. Environ. Eng.* 42, 2139–2146.  
479 <https://doi.org/10.1080/10934520701629617>

480 Larson, A.C., Dreele, R.B.V., 2000. General Structure Analysis System (GSAS) 86–748.

481 Li, C.-Y., Rees, L.V.C., 1986. The thermal stability of faujasites with different Si/Al ratios. *Zeolites* 6,  
482 60–65. [https://doi.org/10.1016/0144-2449\(86\)90013-8](https://doi.org/10.1016/0144-2449(86)90013-8)

483 Li, X., Wu, P., 2017. Geochemical characteristics of dissolved rare earth elements in acid mine  
484 drainage from abandoned high-As coal mining area, southwestern China. *Environ. Sci.*  
485 *Pollut. Res.* 24, 20540–20555. <https://doi.org/10.1007/s11356-017-9670-5>

486 Lie, J., Liu, J.-C., 2021. Selective recovery of rare earth elements (REEs) from spent NiMH batteries  
487 by two-stage acid leaching. *J. Environ. Chem. Eng.* 9.  
488 <https://doi.org/10.1016/j.jece.2021.106084>

489 Mao, F., Zhu, N., Zhu, W., Liu, B., Wu, P., Dang, Z., 2022. Efficient recovery of rare earth elements  
490 from discarded NdFeB magnets by mechanical activation coupled with acid leaching.  
491 *Environ. Sci. Pollut. Res.* 29, 25532–25543. <https://doi.org/10.1007/s11356-021-17761-3>

492 Mondale, K.D., Carland, R.M., Aplan, F.F., 1995. The comparative ion exchange capacities of  
493 natural sedimentary and synthetic zeolites. *Miner. Eng., Minerals Engineering '94*  
494 *Proceedings of the International Conference* 8, 535–548. [https://doi.org/10.1016/0892-](https://doi.org/10.1016/0892-6875(95)00015-1)  
495 [6875\(95\)00015-1](https://doi.org/10.1016/0892-6875(95)00015-1)

- 496 Mosai, A.K., Chimuka, L., Cukrowska, E.M., Kotzé, I.A., Tutu, H., 2019. The Recovery of Rare Earth  
497 Elements (REEs) from Aqueous Solutions Using Natural Zeolite and Bentonite. *Water. Air.*  
498 *Soil Pollut.* 230. <https://doi.org/10.1007/s11270-019-4236-4>
- 499 Mosai, A.K., Tutu, H., 2021. Simultaneous sorption of rare earth elements (including scandium and  
500 yttrium) from aqueous solutions using zeolite clinoptilolite: A column and speciation study.  
501 *Miner. Eng.* 161. <https://doi.org/10.1016/j.mineng.2020.106740>
- 502 Motsi, T., Rowson, N.A., Simmons, M.J.H., 2009. Adsorption of heavy metals from acid mine  
503 drainage by natural zeolite. *Int. J. Miner. Process.* 92, 42–48.  
504 <https://doi.org/10.1016/j.minpro.2009.02.005>
- 505 Opare, E.O., Struhs, E., Mirkouei, A., 2021. A comparative state-of-technology review and future  
506 directions for rare earth element separation. *Renew. Sustain. Energy Rev.* 143.  
507 <https://doi.org/10.1016/j.rser.2021.110917>
- 508 Pavón, S., Fortuny, A., Coll, M.T., Sastre, A.M., 2018. Rare earths separation from fluorescent lamp  
509 wastes using ionic liquids as extractant agents. *Waste Manag.* 82, 241–248.  
510 <https://doi.org/10.1016/j.wasman.2018.10.027>
- 511 Pinto, J., Colónia, J., Abdolvaseei, A., Vale, C., Henriques, B., Pereira, E., 2023. Algal sorbents and  
512 prospects for their application in the sustainable recovery of rare earth elements from E-  
513 waste. *Environ. Sci. Pollut. Res.* 30, 74521–74543. [https://doi.org/10.1007/s11356-023-](https://doi.org/10.1007/s11356-023-27767-8)  
514 [27767-8](https://doi.org/10.1007/s11356-023-27767-8)
- 515 Porvali, A., Wilson, B.P., Lundström, M., 2018. Lanthanide-alkali double sulfate precipitation from  
516 strong sulfuric acid NiMH battery waste leachate. *Waste Manag.* 71, 381–389.  
517 <https://doi.org/10.1016/j.wasman.2017.10.031>
- 518 Rees, L.V.C., 1970. Chapter 9. Ion exchange in zeolites. *Annu Rep Prog Chem Sect Gen Phys Inorg*  
519 *Chem* 67, 191–212. <https://doi.org/10.1039/GR9706700191>

520 Sánchez-Hernández, R., Padilla, I., López-Andrés, S., López-Delgado, A., 2018. Al-Waste-Based  
521 Zeolite Adsorbent Used for the Removal of Ammonium from Aqueous Solutions. *Int. J.*  
522 *Chem. Eng.* 2018, e1256197. <https://doi.org/10.1155/2018/1256197>

523 Scherzer, J., Bass, J.L., Hunter, F.D., 1975. Structural characterization of hydrothermally treated  
524 lanthanum Y zeolites. I. Framework vibrational spectra and crystal structure. *J. Phys. Chem.*  
525 79, 1194–1199. <https://doi.org/10.1021/j100579a010>

526 Schüßler, F., Pidko, E.A., Kolvenbach, R., Sievers, C., Hensen, E.J.M., Van Santen, R.A., Lercher, J.A.,  
527 2011. Nature and Location of Cationic Lanthanum Species in High Alumina Containing  
528 Faujasite Type Zeolites. *J. Phys. Chem. C* 115, 21763–21776.  
529 <https://doi.org/10.1021/jp205771e>

530 Silva, R.G., Morais, C.A., Teixeira, L.V., Oliveira, É.D., 2019. Selective Precipitation of High-Quality  
531 Rare Earth Oxalates or Carbonates from a Purified Sulfuric Liquor Containing Soluble  
532 Impurities. *Min. Metall. Explor.* 36, 967–977. <https://doi.org/10.1007/s42461-019-0090-6>

533 Xie, B., Liu, C., Wei, B., Wang, R., Ren, R., 2023. Recovery of rare earth elements from waste  
534 phosphors via alkali fusion roasting and controlled potential reduction leaching. *Waste*  
535 *Manag.* 163, 43–51. <https://doi.org/10.1016/j.wasman.2023.03.029>

536 Yang, Y., Walton, A., Sheridan, R., Güth, K., Gauß, R., Gutfleisch, O., Buchert, M., Steenari, B.-M.,  
537 Van Gerven, T., Jones, P.T., Binnemans, K., 2017. REE Recovery from End-of-Life NdFeB  
538 Permanent Magnet Scrap: A Critical Review. *J. Sustain. Metall.* 3, 122–149.  
539 <https://doi.org/10.1007/s40831-016-0090-4>

540 Yantasee, W., Fryxell, G.E., Addleman, R.S., Wiacek, R.J., Koonsiripaiboon, V., Pattamakomsan, K.,  
541 Sukwarotwat, V., Xu, J., Raymond, K.N., 2009. Selective removal of lanthanides from  
542 natural waters, acidic streams and dialysate. *J. Hazard. Mater.* 168, 1233–1238.  
543 <https://doi.org/10.1016/j.jhazmat.2009.03.004>

- 544 Yuksekdag, A., Kose-Mutlu, B., Zeytuncu-Gokoglu, B., Kumral, M., Wiesner, M.R., Koyuncu, I., 2022.  
545 Process optimization for acidic leaching of rare earth elements (REE) from waste electrical  
546 and electronic equipment (WEEE). *Environ. Sci. Pollut. Res.* 29, 7772–7781.  
547 <https://doi.org/10.1007/s11356-021-16207-0>
- 548 Zhang, B., Liu, C., Li, C., Jiang, M., 2014. A novel approach for recovery of rare earths and niobium  
549 from Bayan Obo tailings. *Miner. Eng.* 65, 17–23.  
550 <https://doi.org/10.1016/j.mineng.2014.04.011>
- 551 Zhu, L., Seff, K., 1999. Reinvestigation of the Crystal Structure of Dehydrated Sodium Zeolite X. *J.*  
552 *Phys. Chem. B* 103, 9512–9518. <https://doi.org/10.1021/jp991817l>